Ammonium dihydrogen phosphate doped potassium sulphate single crystals

A Rathika
A Arun Kumar

Ammonium dihydrogen phosphate doped potassium sulphate single crystals

LAP LAMBERT Academic Publishing

A Rathika
A Arun Kumar

Ammonium dihydrogen phosphate doped potassium sulphate single crystals

Contents

Imprint
Any brand names and product names mentioned in this book are subject to trademark, brand or patent protection and are trademarks or registered trademarks of their respective holders. The use of brand names, product names, common names, trade names, product descriptions etc. even without a particular marking in this work is in no way to be construed to mean that such names may be regarded as unrestricted in respect of trademark and brand protection legislation and could thus be used by anyone.

Cover image: www.ingimage.com

Publisher:
LAP LAMBERT Academic Publishing
is a trademark of
Dodo Books Indian Ocean Ltd., member of the OmniScriptum S.R.L Publishing group
str. A.Russo 15, of. 61, Chisinau-2068, Republic of Moldova Europe
Printed at: see last page
ISBN: 978-620-3-85675-0

CHAPTER I

INTRODUCTION

1.1 CRYSTAL GROWTH – AN INTRODUCTION

A systematic and scientific study of crystals including process of crystallization, internal structure, external morphology, properties and classification of crystals is known as "Crystallography". The study of the formation of crystals is covered under the subhead "Crystal Growth". Crystals are made up of regular and periodic three-dimensional patterns of atoms in space. Fundamental experimental aspects of crystal growth were derived from early crystallization in the 18^{th} and 19^{th} century. The critical one to achieve higher quality crystal and the role of transport phenomena was a unique feature of the 20^{th} century. Thus, crystals are considered the pillars of modern technology. Material science is primarily concerned with the fundamental understanding of materials and is ultimately responsible for many of the recent technological innovations [Ballman *et al.*, 1963, Buckley, 1951]. High-efficiency white light-emitting diodes for energy-saving illumination and photovoltaic/thermo-photovoltaic devices for energy conversion with high yield depend on significant advances in crystal growth.

In the past few decades, there has been a growing interest on single crystal growth processes, particularly in view of the increasing demand on materials for technological applications (Brice, 1986). Atomic arrays that are periodic in three dimensions, with repeated distances are called single crystals. It is clearly more difficult to prepare single crystal than polycrystalline material and extra effort is justified because of the outstanding advantages of single crystals (Laudise *et al.*,

1975). The reason for growing single crystal is, many physical properties of solids are obscured or complicated by the effect of grain boundaries. The chief advantages are the anisotropy, uniformity of composition and the absence of boundaries between individual grains, which are inevitably present in polycrystalline materials.

On the basis of the symmetric elements, all crystals come under seven broad systems (ie., cubic, hexagonal, tetragonal, orthorhombic, monoclinic, triclinic, trigonal). The definite ordered arrangement of the faces and edges of a crystal is known as crystal symmetry. If all the atoms at the lattice points are identical, the lattice is called a Bravais lattice.

Therefore, researchers worldwide have always been in search of new materials through their single crystal growth. Single crystals are important in science; thus, they have various invaluable properties such as those of semiconductors, ferroelectrics, dielectrics and so on.

Currently, most of the published research has focused on semi organic crystals to enhance the nonlinear optical properties. Due to familiar properties of both inorganic and organic hosts, until now, semi organic materials have been grown for more familiar broad applications such as frequency modulation, data storage technology, fibre optic communication, optical modelling and electro-optic modulations, because of their good mechanical strength, high optical transmittance, large damage threshold, chemical stability, etc.

1.2 NONLINEAR OPTICAL CRYSTALS

Nonlinear optical (NLO) crystals play a vital role in great impact on laser science and industrial applications. The new development of techniques for the fabrication and growth of artificial materials used for NLO applications has

appreciably contributed to this direction. Hence, the aim is to develop materials presenting large nonlinearities and satisfying the technological requirements for device fabrication. The basic requirements for optical device fabrication include wide transparency range, fast response and high laser damage threshold, etc. In addition to the processability, adaptability and interfacing with other materials, improvement in nonlinear optical device fabrication has led the way to the study of new NLO effects and the introduction of new concepts.

The NLO materials can be classified into three following categories on the basis of cohesive forces.

1. Inorganic crystals
2. Organic crystals
3. Semiorganic crystals

1.2.1 Inorganic Crystals

Inorganic materials are preferred for NLO applications over organic materials. In the beginning, research interest was focused on inorganic materials such as Quartz [Walker and Buehler, 1950], Potassium dihydrogen phosphate (KDP) [Mullin and Amatavivadhana, 1967], Lithium niobate ($LiNbO_3$) [Carruthers *et al.*, 1971], Potassium titanyl phosphate (KTP) [Bolt and Bennema, 1990] etc. Many of these crystals have been successfully used in commercial frequency doublers, mixers, electro-optic modulators and optical parametric oscillators. In particular, KDP and deuterated KDP crystals are widely used as the second, third and fourth harmonic generators for Nd:YAG laser source.

1.2.2 Organic Crystals

The search for organic NLO materials has been increasing in the last few decades because of their potential applications in optical data storage devices. The basic structure of organic NLO materials is based on the π bond system, due to the overlap of π orbitals, delocalization of electronic charge distribution leads to a high mobility of the electron density. However there are some drawbacks with organic NLO materials. As with many other organic solids, the intermolecular forces are comparatively weak, being predominantly vander waals or permanent dipole-dipole interactions. This typically results in low melting point and relatively high vapour pressure. Mechanical properties are, in general, rather poor with most organic solids being relatively soft. This can have important consequences for the structural perfection of the crystals.

1.2.3 Semiorganic Crystals

The inherent limitations on the maximum attainable nonlinearity inorganic materials and the moderate success in growing device grade organic single crystals have made scientists adopt newer strategies. The obvious one is to develop hybrid inorganic-organic materials with little trade-off in their respective advantages. This new class of materials has come to be known as the semiorganics. Semiorganics are primarily classified into two categories, type-I and type-II. Type-I semiorganics are inorganic salts of large conjugated organic molecules. Type-II semi organics are coordination complexes of polarizable organics bonded to metal atoms. The metal atoms help in forming relatively strong coordinate bonds resulting in better thermal and mechanical stabilities. Zinc tris (thiourea) sulphate belongs to this class, with zinc bonded to three thiourea molecules and a sulphate ion. One of the advantages of semi

organics is that the bonding schemes are three dimensional, unlike polar organic crystals and hence result in stubbier habit. Presently, inorganic and organic materials are replaced by semi organic materials. This is due to the development of the mechanical and thermal properties along with good second harmonic generation (SHG) efficiency.

1.3 APPLICATION OF NLO CRYSTALS

For optical applications a nonlinear material should have the following characteristics:

- High optical transparency in the entire visible region
- Non hygroscopic nature
- Higher laser damage threshold
- Be readily available as large single crystals
- Wide phase matching angle
- Ease of fabrication
- High mechanical strength and thermal stability
- Ability to process into crystals and fast optical response

1.4 IMPORTANCE OF THE PRESENT WORK

1.4.1 Potassium Sulphate (K_2SO_4)

K_2SO_4 is also called sulphate of potash arcanite or archaically known as potash of sulfur. It is a non-flammable white crystalline salt. The chemical compound is commonly used in fertilizers, providing both potassium and sulfur. K_2SO_4 is an interesting metal organic compound. The potassium sulphate can be separated some of these minerals like kainite, because the corresponding salt is less soluble in water. The crystal structure of K_2SO_4 is reported by [Goeder, 1928]. Since K_2SO_4 is known

to be ionized in solution into K^+ ions and SO_4^- ions and since other inorganic crystals which can be grown from ionic solutions have been shown to preserve their ions in the crystal structure. Several researchers have carried out a lot of studies on large crystals of pure and doped K_2SO_4 were grown from aqueous solution by slow evaporation solution technique (SEST) method. Potassium sulphate is very often used in the NLO studies [Ramasamy *et al.*, 2012]. The XRD study revealed that the structure of urea doped with potassium sulfate are slightly distorted compared to the pure potassium sulphate crystal. The spectral analysis and conductivity studies were reported by authors [Radhika *et al.*, 2013, Sunila Vasi *et al.*, 2014, Vanitha Duraikkan *et al.*, 2012]. In pure K_2SO_4, the effect of mixing some dopants have also been studied by authors. Growth and characterization of pure and Ni^{2+} added glycine potassium sulfate single crystals, cupric ion and iron ion doped in the K_2SO_4 crystal was reported by [Karolin *et al.*, 2013, Tariq *et al.*, 2016].

PROPERTIES	
Molecular Formula	K_2SO_4
Molar Mass	174.259 g/mol
Appearance	White solid
Density	2.66 g/cm^3
Melting Point	1069°C
Boiling Point	1689°C
Solubility	Soluble in water

1.4.2 Ammonium Dihydrogen Phosphate (ADP)

ADP is an interesting inorganic material, hydrogen-bonded compound, belongs to isomorphous series of phosphates and arsenates that presents a strong piezoelectric, dielectric, antiferroelectric properties, nonlinear optical properties and parametric generator [Marder *et al.*, 1991, Voronov *et al.*, 2011]. ADP belongs to the tetragonal system. These molecular crystals exhibit low-temperature order-disorder phase transitions. ADP is widely used as the second, third and fourth harmonic generator for Nd:YAG and Nd:YLF lasers, Applications of integrated electro-optics include high-speed modulation and switching of optical signals for telecommunications and signal processing [Dongfeng *et al.*, 2005]. Several researchers have carried out a lot of studies on large crystals of pure ADP were grown from aqueous solution by temperature lowering method [Li *et al.*, 2001, Xu *et al.*, 2008]. ADP single crystals were grown by gel method using sodium metasilicate (SMS) [Sunil Chaki *et al.*, 2012]. Good quality ADP single crystals have been grown using the uniaxially solution-crystallization method of Sankaranarayanan–Ramasamy (SR) method and SR method with slotted ampoule has been reported by [Sethuraman *et al.*, 2006, Rajesh *et al.*, 2009] and good quality ADP–KDP mixed crystal [Rajesh *et al.*, 2011] grown by slow cooling method. Pure and urea added ADP crystal [Ananthi *et al.*, 2011]. Investigation on the linear and nonlinear optical properties of L-Lysine, L-Malic acid doped ADP crystal for NLO Applications [Shaikh *et al.*, 2014] [Arulmani *et al.*, 2017] have been grown by SEST method.

PROPERTIES	
Molecular Formula	$NH_4H_2PO_4$
Molar Mass	115.03 g/mol
Appearance	White
Density	2.5314 g/cm^3
Melting Point	190-204 °C
Boiling Point	Not applicable
Solubility	Soluble in water

1.5 AIMS AND OBJECTIVES

While considerable amount of information has been obtained through the detailed investigation of the chosen system, the search and design of high efficient nonlinear optical (NLO) crystals for visible and ultraviolet (UV) regions are extremely important for laser and material processing. An attempt has been made to grow some nonlinear optical crystals.

The present investigation is aimed to :

- Grow bulk sized ADP doped K_2SO_4 single crystals.
- Identify the crystal structure by single crystal and powder X-ray diffraction analyses.
- Confirm the various functional groups present in the grown crystal through the FT-IR spectra.
- Estimate the transmission range, band gap, extinction coefficient, refractive index and reflectance of the crystal by UV-Vis spectra.
- Study the thermal behaviour of the grown crystals by TGA/DTA.

- Estimate the mechanical strength of the crystal by Vicker's hardness tester.
- Check the nonlinear response of the crystal by incident coherent LASER light (Kurtz and Perry powder technique).

1.6 SCOPE OF THE PRESENT WORK

In recent years, much attention has been paid to the research of inorganic crystals. Doping is possible if a suitable host can be found. Due to useful applications of doping, in the present study, the investigations are focused on growth and characterization of ADP doped K_2SO_4 compound at room temperature. The doping crystals can alter various physical and chemical properties and find wide applications in optoelectronic devices compared to pure crystals.

CHAPTER II

REVIEW OF LITERATURE

Currently, most of the published research has focused on semiorganic crystals to enhance the nonlinear optical properties. Due ,to familiar properties of both inorganic and organic hosts, until now, semiorganic materials have been grown for more familiar broad applications, such as frequency modulation, data storage technology, fibre optic communication, optical modelling and electro-optic modulations, because of their good mechanical strength, high optical transmittance, large damage threshold, chemical stability, etc.

Related to the work carried out in this report, literature review was done on the growth of crystals by solution growth technique in order to understand the experimental details, growth procedures, the nature and the effects of solvents.

Goeder, 1928 has reported the crystal structure and the elementary lattice of K_2SO_4. It contains four molecules and the lattice constants are a = 5.746 Å, b = 10.033 Å, c = 7.443 Å and the system is orthorhombic. Since K_2SO_4 is known to be ionized in solution into K^+ ions and SO_4^- ions and since other inorganic crystals which can be grown from ionic solutions have been shown to preserve their ions in the crystal structure and also determine the orientation of the oxygen nuclei with respect to the sulphur.

Li *et al.*, 2001 has reported the large crystals of ADP were grown from aqueous solution by temperature lowering method. The electro-optical coefficients were measured by the static method at wavelengths of 632.8 and 488 nm. The experimental results indicated that the crystals have good optical quality.

Sethuraman *et al.*, 2006 has determined the unidirectional growth of (110) ADP single crystal by SR method. Various crystal growth methods like solution growth method, Bridgeman Stockbarger method, Czochralski method are employed to grow bulk size crystals. The growth conditions were optimized for 20 mm diameter crucible with growth solution. The grown crystal has transparency range from 400-1100 nm with transmittance of 60%.

Rajesh *et al.*, 2009 has reported the optical, dielectric and microhardness studies on (100) directed ADP crystal by the uniaxially solution crystallization method of SR. The size of the grown crystal is 40 mm in diameter and 50 mm in thickness. Dielectric measurement reveals the dielectric constant is high and dielectric loss is low in SR grown crystal compared to the crystal grown by conventional method.

Ananthi *et al.*, 2011 has reported urea added ADP single crystals by slow evaporation technique. Crystallinity of the pure and doped crystal has been studied by XRD analysis. FT-IR studies confirm the functional group of the crystals. TGA/DTA confirm that decomposition temperatures of the doped crystals have been decreased.

Rajesh *et al.*, 2011 has grown the ADP-KDP mixed crystal and its optical, mechanical, dielectric, piezoelectric and laser damage threshold studies by slow cooling method. HR-XRD studies have been done in the near and far regions of the seed crystal. In the UV-Vis spectra, 80% of transparency is observed in the entire visible region. Vicker's hardness studies indicate that the mixed crystal is mechanically more stable compared to the ADP. Higher piezoelectric coefficient is observed in mixed crystal.

Ramasamy *et al.*, 2012 has grown the synthesis, characterization, crystal structure and NLO properties of a new mixed crystal ADP. KDP, sodium dihydrogen phosphate by slow evaporation technique. Crystal composition is determined by single crystal XRD analysis reveals that it belongs to the tetragonal system with non centrosymmetric phase group. The presence of sodium and potassium in ADP matrix was confirmed by ICPES and EDAX spectroscopy.

Sunil chaki *et al.*, 2012 has reported the growth and characterization of ADP single crystal by gel method using SMS. The XRD analysis showed that it passes tetragonal structure having lattice parameters a = 7.502 Å, c = 7.554 Å. The FT-IR spectra showed peaks due to vibration and stretching. The UV-Vis-NIR spectroscopy showed direct optical band gap of 4.99 eV and indirect optical band gap of 4.12 eV.

Vanitha Duraikkan *et al.*, 2012 has reported the crystal growth and characterization of potassium manganese nickel sulfate hexahydrate (KMNNSH)-A new UV filter by traditional slow evaporation method. The grown crystals were confirmed by XRD analysis. FT-IR confirmed the presence of water molecule and sulfate group. The UV-Vis study confirms the doped crystal filter blocks the unwanted transmission in the range 400-1000 nm ranges and hence acts as efficient filter. The thermal analysis indicates the water molecules are present in the KMNNSH crystals. AAS confirmed the presence of Mn atoms in the expected stoichiometry.

Karolin *et al.*, 2013 has reported the pure and Ni^{2+} added glycine potassium sulphate (GPS) single crystals were grown by slow evaporation technique. Crystalline nature of the pure and doped crystals has been studied by XRD analysis. FT-IR spectra were recorded by the KBr pellet method in the wavenumber range 400-4000 cm^{-1}. The UV-Vis-NIR absorption spectra were recorded in the wavelength range

1900-1400 nm. The mechanical behaviour has been assessed by Vicker's microhardness measurements and [illegible] crystals have been tested by Kurtz and Perry powder technique.

Radhika *et al.*, 2013 has reported the growth, optical, thermal, mechanical and dielectric studies of potassium sulfate crystals doped with urea by SEST method. Single crystal XRD analysis confirms orthorhombic crystal structure. Powder XRD pattern confirms that the grown crystals possess high crystalline nature. Vibrational spectrum reveals the symmetric of molecule. The crystal have a lower cut-off wavelength of 384 nm. The dielectric constant and dielectric loss were calculated by varying frequencies temperatures between 25°C and 45°C.

Shaikh *et al.*, 2014 has reported the investigation of L-lysine doped ADP crystal has been grown by slow evaporation technique. The crystalline nature of the grown crystal was confirmed by powder XRD technique. The optical studies were carried to examine transparency and band gap of crystal is found to be 4.7 eV. The third order nonlinear behaviour has been investigated using Z-scan technique at 632.8 nm. The nonlinear third order susceptibility of grown crystal is found to be 1 .578 x 10^{-5}esu. The nonlinear index of refraction and absorption coefficient were determined by Kurtz powder test.

Sunila Vasi *et al.*, 2014 has reported the investigation on the growth and properties of $(LA)_x(K_2SO_4)_{1-x}$ single crystals by slow evaporation method. The grown crystals were subjected to single crystal XRD analysis. The FT-IR spectrum was recorded in the range of 4000-450 cm^{-1}. The concentration has not affect the optical absorbance in the entire visible range. The electrical parameters of the single crystals

were determined by AC measurement for various frequencies. SHG efficiency of the grown crystal were confirmed by Kurtz powder method.

Tariq *et al.*, 2016 has determined the dielectric and optical behaviour of pure potassium sulfate and doped with copper and iron. The dielectric constant and its loss of K_2SO_4 and doped samples decreases with frequency increases, while its UV-Vis spectra confirmed that the doped sample filter blocks the unwanted transmission and hence act as efficient filter. Energy gap of pure K_2SO_4 and doped with copper and iron ions were found to be 5.9 eV and 6.048 eV respectively, which is reasonable for typical dielectric materials. The lower cut-off wavelength is 385 nm and this property is used for nonlinear optical applications.

Arulmani *et al.*, 2017 has investigated the L-Malic acid doped ADP (LMADP) single crystals were grown by slow evaporation method at room temperature. The Crystalline nature of the grown crystal has been studied by powder XRD analysis. A FT-IR study confirms the functional groups of the crystals. The UV-Vis study confirms the wide optical transmittance window for the doped crystals imperative for optoelectronics applications. TG/DTA analyses were carried out to characterize the melting behaviour and stability. The electrical properties of the grown crystal have been analyzed by dielectric constant and dielectric loss with frequency. The SHG efficiency of the crystal was determined by NLO studies.

CHAPTER III

THEORETICAL CONCEPTS AND METHODOLOGY

Crystal growth is an art, and there are many variations to the basic crystal growing recipes as there are crystallographers. Growth of crystal ranges from a small inexpensive technique to a complex sophisticated expensive process. The crystallization time ranges from minutes, hours, days and to months.

Producing good quality crystals of a suitable size is the first and most important step in determining any crystal structure. Crystallization is the process of arranging atoms or molecules that are in a fluid or solution state into an ordered solid state.

There are two major stages involved in the crystallization process,

- Nucleation
- Crystal growth

3.1 NUCLEATION

The crystal growth process starts with the nucleation stage. Nucleation is the first step in growing a single crystal from a mother solution. The formation of nuclei or embryos in the solution is often termed the centre of crystallization. Nucleation is the stage where crystal forming units (atoms, ions or molecules) gather into clusters which are unstable until they reach a critical size. Stable clusters are called nuclei which have three dimensional formation [Scheel, 2003].

The fundamental process of nucleation is classified as two categories

1. Homogeneous nucleation
2. Heterogeneous nucleation

3.1.1 Homogeneous Nucleation

The spontaneous formation of crystalline nuclei in the interior of the parent phase contains no impurities is called homogeneous nucleation.

3.1.2 Heterogeneous Nucleation

In heterogeneous nucleation, the parent material contains impurities. Here, the foreign particles induce crystallization within the parent material, which is faster than homogeneous nucleation. The advantage of heterogeneous nucleation is a short processing time to crystallization with simplicity, as it is common to add foreign substances such as string or rock to the solution [Ballman *et al.*, 1963].

Both these nucleation are called primary nucleation and occur in systems that do not contain crystalline matter. On the other hand, nuclei are often generated in the vicinity of crystals present in the supersaturated system. This phenomenon is referred to as secondary nucleation. Growth of crystals from solutions can occur if some degree of supersaturation or supercooling has been achieved first in the system.

The growth of crystals can be considered in three basic steps involved in the crystallization process:

- Achievement of supersaturation or supercooling.
- Formation of crystal nuclei of microscopic size.
- Successive growth of crystals to yield distinct faces.

3.2 CRYSTAL GROWTH TECHNIQUES

Crystals grow by the ordered deposition of material from the fluid or solution state to a surface of the crystal. There are numerous ways to grow crystals. The choice of method depends greatly upon the physical and chemical properties of the sample. Single crystals may be produced by the transport of crystal constituents in the solid,

liquid or vapour phases. Phase change transitions are significant for crystal growth techniques. On the basis of this, crystal growth may be classified into three main categories.

1. Melt growth (growth from molten liquid to solid)
2. Vapour growth (growth from vapour to solid)
3. Solution growth (growth from liquid to solid)

In the above mentioned categories liquid growth includes both melt and solution growth processes. A survey on the methods of crystal growth suggests that almost 80% of the single crystals are grown from the melt compared with roughly 5% from vapour, 5% from low temperature solution, 5% from high temperature solution, and 3% from the solid and only 2% by hydrothermal methods [Brice, 1986].

3.3 GROWTH FROM SOLUTION

Growth of crystals from aqueous solution is one of the most ancient methods of crystal growth. Crystal growth from solution is very important process used in many applications from laboratory to industry. Materials which decompose on heating or which exhibit structural transformations while cooling from the melting point can be grown from the solution growth method if suitable solvents are available. This method is more widely used to grow bulk crystals [Santhanaraghavan and Ramasamy, 2002]. Growth from solution, however, is used more broadly because, compared with growth from the melt technique, it requires lower temperatures and can lead to lower density of lattice defects. The growth from low temperature solution involves much more time.

3.3.1 Advantages of Solution Growth

- The growth process occurs near the ambient temperature.

- Growth apparatus is relatively simple and cheap
- The concentration of structural imperfections in solution grown crystals is relatively low.
- Sometimes, impurities may slow down the crystallization process by being adsorbed on the growing face of the crystal which changes the crystal habit
- Low temperature introduces small thermal stress in the grown crystals

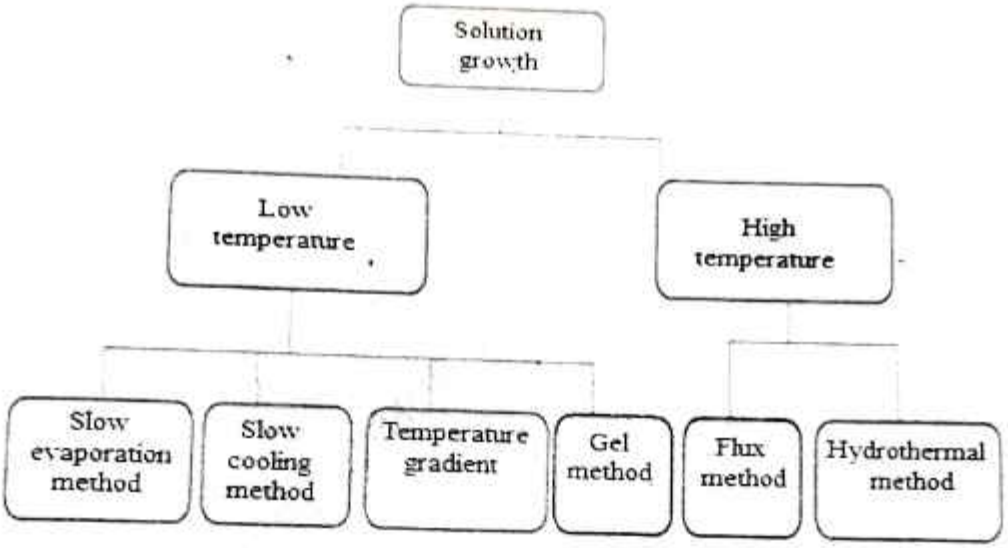

Depending on the solvents and the solubility of the solute. Solution growth can be classified into

1. Low temperature solution growth
2. High temperature solution growth

Among the various methods of growing single crystals, solution growth at low temperatures occupies a prominent place owing to its versatility and simplicity. After undergoing so many modifications and refinements, the process of solution growth now yields good quality crystals for a variety of applications.

3.4 LOW TEMPERATURE SOLUTION GROWTH

Low temperature solution growth is the simplest and in many cases the least expensive method for production of optical crystals. However, its use for growth of large commercially important single crystals has been limited in the past several years to a few inorganic and organic materials. The method of crystal growth from low temperature aqueous solutions is extremely popular in the production of many technologically important crystals. The growth of materials by low temperature solution growth involves weeks, months and even years sometimes. A solvent with less viscosity is preferable. The low temperature solution growth technique is well suited to those materials which suffer from decomposition in the melt or in the solid at high temperatures and which undergo structural deformations while numerous organic and inorganic materials, which fall in this category can be crystallized using this technique. This technique also allows a variety of different morphologies and polymorphic forms of the same substance which can be grown by varying the growth conditions. Among the various methods of growing single crystals, the solution growth at low temperatures occupies a prominent place owing to its versatility and simplicity. After undergoing so many modifications and refinements, the process of solution growth now yields good quality crystals for a variety of applications [Byrappa and Ohachi, 2003, Kumar and Tadson, 2007, Santhanaraghavan and Ramasamy, 2002].

Low temperature solution growth can be subdivided as follows:

1. Slow evaporation solution technique
2. Slow cooling method
3. Temperature gradient method

3.4.1 Slow Evaporation Solution Technique (SEST)

Generally, crystallization of salt was achieved by the evaporation of water from the solution, which in contemporary times is called the solvent evaporation method [Bhat, 2015]. Evaporation is by far one of the easiest methods for crystallizing organic and organometallic small molecule compounds. The rate of crystal growth can be controlled either by reducing the rate of evaporation of the solvent or by cooling the solution. The number of nucleation sites may be increased either by seeding the solution or by scratching the exposed surfaces of the glass vessel. In this method, an excess of a given solute is established by utilizing the difference between the rates of evaporation of the solvent and the solute. In the solvent evaporation method, the solution loses particles which are weakly bound to other components and therefore, the volume of the solution decreases. The vapour pressure of the solvent is high and evaporates more rapidly and the solution becomes supersaturated [Chernov, 1984].

3.5 OPTIMIZING SOLUTION GROWTH

3.5.1 Solution, Solubility and Supersolubility

A solution is a homogeneous mixture of a solute and a solvent. Solute is the component which is present in a smaller quantity and that one which gets dissolved in the solution. For a given solute, there may be different solvents. A good solvent ideally displays the following characteristics:

a) Moderate solubility

b) A small vapour pressure

c) Non-corrosiveness

d) Non-toxicity

e) Non-flammability

f) Less volatility

It is known that the choice of solvent provides some control over crystal habit and this effect depends on the interaction of the surface of the crystal as it grows and the solvent molecules. Also this effect is related to the influence of impurities or additives. Solvents commonly used include deionized water, both light (H_2O) and heavy (D_2O), ethanol, methanol, acetone, carbon tetrachloride, hexane, xylene and many other solvents having the similar characteristics. Almost 90% of the crystals from low temperature solution are grown by using water as a solvent.

Solubility gradient is another important parameter which dictates the growth procedures. If the solubility is too high, it is difficult to grow bulk single crystals and the size and growth rate of the crystals are restricted for low solubility.

Supersaturation is important parameter for the solution growth process. The crystal growth by the accession of the solute in the solution as a degree of supersaturation is maintained. Hence the solubility of the solute may be determined by dissolving the solute in the solvent maintained at a constant temperature with continuous stirring.

3.5.2 Preparation of Solution

For solution preparation it is essential to have the solubility data of the material at different temperatures. Sintered glass filters of different pore size are used for solution filtration. The clear solution, saturated at the desired temperature is taken in a growth vessel. A small crystal suspended in the solution is used to test the saturation. The test seed is replaced with a good quality seed. Growth is initiated after

lowering the temperature to the equilibrium saturation. Solvent evaporation can also be helpful in initiating the crystal growth.

3.5.3 Purification Processes

Purification process can be achieved by repeated crystallization of the substance in an appropriate solvent. High purity of raw material is an essential prerequisite for success in crystal growth. Impurities are of considerable importance, not only because of their influence on the physical and chemical properties on the resulting crystals, but also they can play a dominant role in controlling the crystal growth behaviour. Sometimes suspended impurities may slow down the crystallization process by being adsorbed on the surface of the crystal, which changes the crystal habit [Buckley, 1951]. A careful repetitive use of standard purification method of recrystallization followed by filtration of the solution would increase the level of purity. The recrystallization has to be carried out two or three times to ensure optimum purification.

3.5.4 Harvesting of the Grown Crystals

If a crystal is extracted from a solution kept close to the room temperature, it can be dried by means of filter paper. Filter paper must not be used to rub the surface since the majority of crystals prepared from low temperature solutions are easily scratched. The surface of a carelessly treated crystal may acquire many defects. To prevent this, a filter paper and a towel are heated approximately to the temperature of the solution. A crystal should not be touched by hand but a crystal holder should be used to extract it from the crystallizer. Contact with warm and moist fingers may crack a crystal or etch it.

3.5.5 Crystal Perfection

Mostly, all crystals grow approximately at equivalent rates in all dimensions. This will result in a large bulk crystal from which samples of any desired orientation can be cut. The perfection of the final crystal is based on the following

i. The purity of the starting materials
ii. The quality of the seed crystal
iii. Cooling rate employed
iv. The efficiency of agitation

3.6 SLOW COOLING METHOD

This is the best method among all the known methods to grow bulk single crystals from solution. The supersaturation of the systematic cooling requires the volume of the crystallizer finite and the amount of substance in it is limited. So, the volume of the crystallizer is selected based upon the desired size of the crystals and the temperature of the solubility of the substance for a particular temperature. The temperature at which such crystallization can begin is usually in the range 45-70°C and lower limit of cooling is the room temperature [Tareen and Kutty, 1971, Vere, 1987].

3.7 TEMPERATURE GRADIENT METHOD

This method involves the transport of the materials from a hot region containing the source material to be grown to a cooler region where the solution is supersaturated. The main advantages of this method are that

a) Crystal growth at a fixed temperature
b) This method intensitive to changes in temperature provided both the source and the growing crystal undergo the same change.

c) Economy of the solvent and solute

3.8 HIGH TEMPERATURE SOLUTION GROWTH

In high temperature solutions, the constituents of the material to be crystallized are dissolved in a suitable solvent and crystallization occurs as the solution becomes critically supersaturated. The supersaturated may be promoted by evaporation of the solvent, by cooling the solution or by a transport process in which the solute is made to flow from a hotter to a cooler region. The high temperature crystal growth can be divided into two categories

- Growth from single component system
- Growth from multi component system

This method is widely used for the growth of oxide crystals. The procedure is to heat the container having flux and the solute to a temperature. So that all the solute materials dissolve. This temperature is maintaining for a soak period of several hours and then the temperature is lowered very slow.

3.9 HYDROTHERMAL GROWTH

Hydrothermal growth means that high pressure, as well as high temperature, is used to solubilize otherwise insoluble materials, such as quartz, calcite, alumina and antimony sulfoiodide, in water. The hydrothermal technique is well suited for materials that otherwise require high temperature crystallization because the temperature is low during growth compared to the melting point of the material. The well known example is quartz, which was reported [Brice, 1986].

3.10 GEL GROWTH

Crystal growth in gels is a promising technique for growing single crystals of substances that are slightly soluble in water and that cannot be grown conveniently

from a melt or vapour. The gel method has also been applied to study crystal formation in vitro. Recently, crystals of biological macromolecules (proteins) have been grown by this method [Hatschek *et al*., 1912].

3.11 GROWTH FROM MELT

All materials can be grown in single crystal form from the melt provided they melt congruently without decomposition at the melting point and do not undergo any phase transformation between the melting point and room temperature. Depending on the thermal characteristics, the following techniques are employed [Santhanaraghavan and Ramasamy, 2000].

1. Bridgman Technique
2. Czochrarski Technique
3. Kyropoulos Technique
4. Zone melting Technique
5. Verneuil Technique

3.12 VAPOUR GROWTH

A suitable technique in crystal growth is the vapour phase method, which is used in electronic and optoelectronic industries. This method can be classified into two categories: physical and chemical vapour deposition. The transport material is deposited in the growth zone from the vapour phase. Cadmium sulphide and cerium telluride crystals have been grown by this method. Some of the studies that have investigated the growth of crystals by CVD and PVD have reported [Semmelroth *et al*., 2007].

3.3 CHARACTERIZATION TECHNIQUES

Instrumentation part is the backbone of crystal research technology. A complete description of the physical and chemical properties of a material is termed as characterization of that material.

3.3.1 X-ray Diffraction

Spectroscopic and resonance techniques play important role. But the most definite structural data have largely been acquired by using diffraction methods. There are two important X-ray diffraction methods namely,

1. Single crystal X-ray diffraction
2. Powder X-ray diffraction

3.3.1.1 Single Crystal X-ray Diffraction

The single crystal X-ray diffraction is a non-destructive analytical technique that is commonly used to determine the structures of new materials.

Principle

In a single crystal XRD experiment, the reciprocal space of a crystal is constructed by measuring the angles and intensities of reflections in observed diffraction patterns [Crundwell *et al.*, 1999, Milburn, 1973]. In the present study, **ENRAF (BRUKER) NONIUS CAD4 single crystal X-ray diffractometer** system equipped with graphite-monochromated MoK_α (λ = 0.71073 Å) radiation is used. Single crystal XRD consists of an FR 590 generator, a goniometer to hold and rotate the crystal, CAD4F interface and a microVAX3100 equipped with a printer and plotter. Instruments typically contain a beam stop to halt the primary X-ray beam from hitting the detector, and a camera to help positioning the crystal. The unit cell dimensions and orientation matrix are determined using atleast 25 reflections and then

the intensity data of a given set of reflections are collected automatically by the computer. The goniometer equipped with the diffractometer is four circle goniometer with φ, χ, ω and 2θ axes by which the crystal is rotated. A single crystal is mounted on a thin glass fiber fixed on the goniometer head using cyanoacrylate. The calculation of the unit cell parameters (a, b, c, α, β & γ), volume and space group etc. The schematic diagram of single crystal XRD is shown in Figure 3.1.

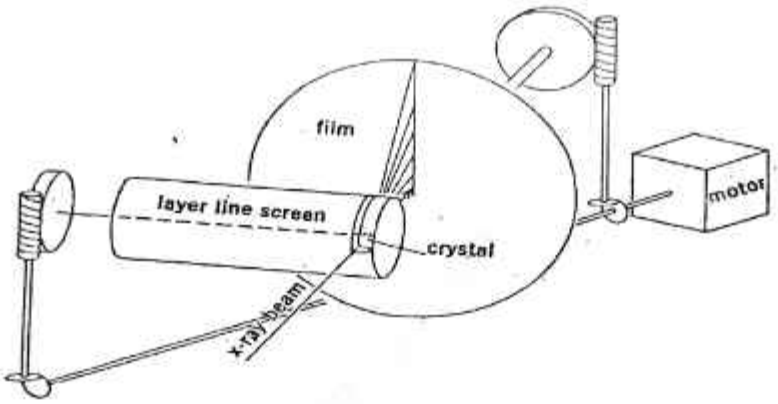

Figure 3.1 Schematic diagram of single crystal XRD

Sample Preparation

The defect free crystal of dimensions around 0.2 x 0.2 x 0.2 mm^3 can be used for the single crystal analysis. The utmost care must be taken to choose the defect free crystal by using a microscope.

Applications

- It can be used to identify the new materials and crystal structural refinement.
- Determination of unit cell, bond lengths, bond angles and site ordering.
- Variations in crystal lattice chemistry etc.

3.3.1.2 Powder X-ray Diffraction

Powder XRD is a rapid analytical technique primarily used for phase identification ("finger print identification") of a crystalline material. This method has been used for quantitative analysis, extraction of three dimensional micro structural properties and determination of the structure imperfections.

Principle

The XRD works on the principle of Bragg's law. According to this law, when a beam of monochromatic X-rays falls on a crystal, each atom becomes a source of scattering radiations. The combined scattering of X-rays from these planes can be considered as a reflection [Clearfield *et al.*, 2008, Vitalij *et al.*, 2009]. The possible d-spacing defined by the indices h, k, l are determined by the shape of the unit cell. Bragg's law gives the relation between the X-ray wavelength λ, d spacing and the angle of incidence θ,

$$n\lambda = 2d \sin \theta$$

Where, n is an integer (1, 2, 3, 4,...etc) which represents the serial order of diffracted beams

λ is the wavelength of the X-ray

d is the interplanar spacing generating the diffraction

θ is the diffraction angle

In the present study, powder XRD was recorded by **XPERT-PRO X-ray diffractometer** system. Figure 3.2 shows the schematic diagram of powder X-Ray diffraction instrument. The sample should be thick enough to ensure that the whole incident X-ray beam interacts with the sample and does not pass through it. When electrons have sufficient energy to dislodge inner shell electrons of the target material,

characteristic X-ray spectra are produced. The specific wavelengths are characteristic of the target material (Cu, Fe, Mo, Cr). Powder X-ray diffractometer is capable of producing a beam of monochromatic X-rays from a CuK_{α} radiation source of wavelength (λ = 1.54060 Å). These X-rays are collimated and directed onto the sample. As the sample and detector are rotated, the intensity of the reflected X-rays is recorded.

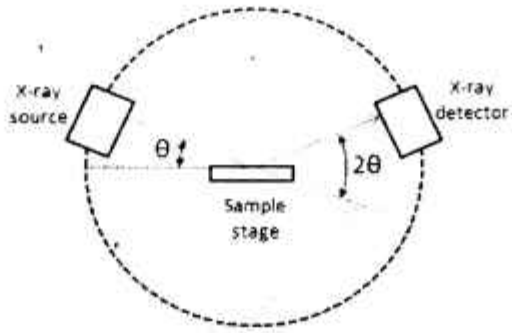

Figure 3.2 Schematic diagram of powder XRD

Sample Preparation

The crystal was subjected to a fine powder using agate mortar and slieved into 1.0 μm slieve. A small amount of this uniform particle size powder is subjected to powder XRD analysis.

Applications

- The X-ray powder diffraction is most widely used for the identification of unknown crystalline material.
- Identification of fine-grained minerals such as clays and mixed layer clays that are difficult to determine optically.

- Investigation of sample stress and strain etc.

3.3.2 Fourier Transform Infrared Spectroscopy (FT-IR Spectroscopy)

FT-IR spectroscopy is a technique used to determine qualitative and quantitative features of IR-active molecules in organic or inorganic solid, liquid or gas samples.

Principle

The IR spectroscopy involves study of the interaction of electromagnetic radiation with matter. Due to this interaction, electromagnetic radiation characteristic of the interacting system may be absorbed or emitted. The absorption bands for most organic and inorganic compounds are found in the IR region. In the present study, vibrational characteristics of the grown sample has been investigated using **8400S Shimadzu infrared spectrophotometer**. Figure 3.3 shows the schematic diagram of FT-IR spectrometer. There are three basic spectrometer components are nernst glower as source, an interferometer chamber and a detector. The interferometer divides radiant beams, generates an optical path difference between the beams and then recombines them in order to produce repetitive interference signals measured as a function of optical path difference by a detector. The interferometer produces interference signals, which contain infrared spectral information generated after passing through a sample. The most commonly used interferometer is a Michelson interferometer which consists of three active components: a moving mirror, a fixed mirror, and a beam splitter. The two mirrors are perpendicular to each other. The beam splitter is a semi reflecting device and is often made by depositing a thin film of germanium onto a flat KBr substrate. Solid samples can be mild with KBr to form a very fine powder. This powder is then compressed into a thin pellet with the help of

pelletizer which can be analyzed. Details of the assignments of different frequencies with different vibrations of bonds, such as OH, NH, NH$_2$, C=O, -CHO, -COOH, NO etc. are given [Bellamy, 1980, Smith, 1999].

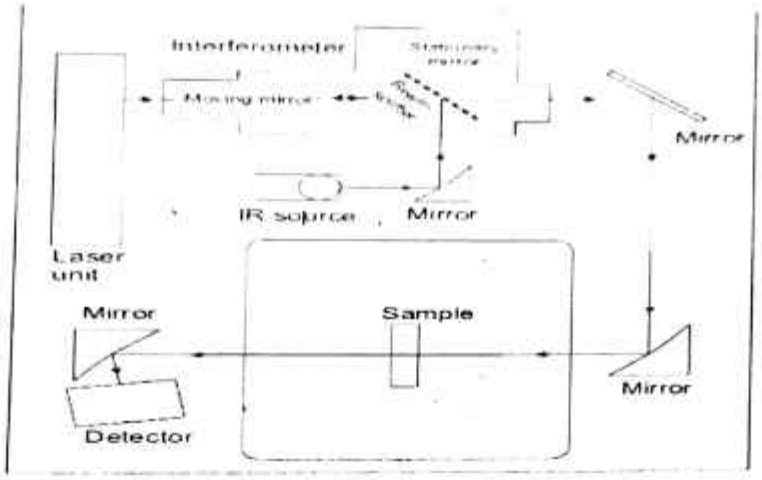

Figure 3.3 Schematic diagram of FT-IR spectrometer

Sample Preparation

The grown crystals are crushed into fine powder by using agate mortar pelletizer. The fine powder of the sample is mild with spectral grade Potassium bromide (KBr) to form a thin pellet using pelletizer, which can be analyzed. KBr is transparent in the IR region.

Applications

- Determination of functional groups in the given materials.
- Unknown materials can be identified.
- Determination of the molecular composition.

3.3.3 Ultraviolet Visible Spectroscopy (UV-Vis Spectroscopy)

UV-Vis spectroscopy is the measurement and interpretation of electromagnetic radiation absorbed or emitted when the molecules or atoms or ions of a sample move from one energy state to another energy state.

Principle

UV-Vis spectroscopy involves the absorption of ultraviolet light by a material and valence (outer) electrons are promoted from their normal (ground) states to higher energy (excited) states. Organic compounds, with a high degree of conjugation, absorb electromagnetic radiation [Sadler *et al.*, 1979]. Valence electrons are found in three types of electron orbitals namely 'σ' bonding orbitals, 'π' bonding orbitals, non-bonding orbitals (n-lone pair electrons) and 'σ^* or π^*' antibonding orbitals. In this investigation, **Perkin Elmer Lambda 35 double beam UV-Vis spectrometer** was used to study the optical quality in the wavelength range of 200–1200 nm. Figure 3.4 shows the schematic diagram of UV-Vis spectroscopy. The basic parts of a spectrometer are a light source, sample holder, a diffraction grating or monochromator to separate the different wavelengths of light and a detector. The UV-Vis spectrophotometer uses two light sources, a deuterium (D_2) lamp for ultraviolet light and a tungsten (W) lamp for visible light. After bouncing off a mirror 1, the light beam passes through a slit and hits a diffraction grating. The grating can be rotated allowing for a specific wavelength to be selected. At any specific orientation of the grating, only monochromatic waves (single wavelength) successfully passes through a slit. One of the beams is allowed to pass through a reference cuvette (which contains the solvent only), the other passes through the sample cuvette. The intensities of the light beams are then measured at the end.

Figure 3.4 Schematic diagram of UV-Vis spectroscopy

Sample Preparation

For UV-Vis spectroscopy, two types can be adopted; one is solid mode and the other is liquid mode. For solid mode, the well ordered crystals of size around 5 x 5 x 2 mm^3 thickness can be used. For liquids, the grown crystal is crushed into fine powder and dissolved in a suitable solvent (deionized water, ethanol, methanol etc).

Applications

- Qualitative and quantitative studies of material can be performed.
- Used to measure the global radiation.
- Used to test optical materials.

3.3.4 Thermal Analysis (TG/DTG)

Thermal analysis is a group of techniques that study the properties of materials as they change with temperature. Thermal analysis gives information regarding phase transition, water of crystallization and different stages of decomposition of the crystal system.

Principle

In the present work, thermal behaviour have been investigated using **NETZSCH STA thermal analyzer**. Figure 3.5 shows the schematic diagram of TGA/DSC. Thermoanalytical incorporates the following three closely related techniques:

1. Thermogravimetric analysis (TGA), which involves monitoring weight while varying temperature.
2. Differential thermal analysis (DTA), which involves comparing the precise temperature difference between a sample and an inert reference material, while heating both.
3. Differential scanning calorimetry (DSC), similar to DTA except that electrical energy is used to restore the cooler of the two materials to the same temperature as the other. This allows direct measurement of energy changes.

Among the thermal methods, the most widely used techniques are TG, DTA which find extensive use in all fields of organic, inorganic chemistry, metallurgy, mineralogy and many other areas. In the present work, thermal behaviour of the grown crystals has been investigated using TG-DTG techniques.

Even though different types of balance mechanism are available today, those employing null-point-weighing mechanism are favoured as the sample remains in the same zone of furnace irrespective of changes in mass. The furnace is normally an electrical resistive heater and the temperature range for most of the furnace is from ambient to 2000°C.

The measuring system consists of two micro furnaces made of Platinum-Iridium alloy, which contains a platinum resistance thermometer as a temperature

sensor and a heating resistor made of platinum wire. Both micro furnaces separated from each other, are positioned in an aluminum block of constant temperature. The maximum heating power of a micro furnace is about 14 W; the maximum heating rate is 500 K/min. The measuring range extends from -175°C to 725°C. During the programmed heating, some heating powder is supplied to both micro furnaces through a control circuit. Whenever a symmetry occurs, a temperature difference results between the furnaces and the system adjusts the power supplied to both the furnaces in such a way that the temperature difference is maintained at zero [Willard *et al.*, 2004].

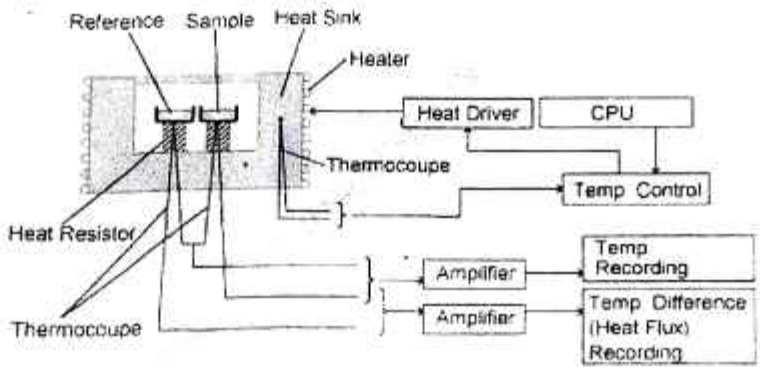

Figure 3.5 Schematic diagram of TGA/DSC

Sample Preparation

The grown crystal is crushed to make powder by agate mortar. When preparing a sample, the size of the sample should be between 2 and 50 mg. The powdered sample was taken in the alumina crucible.

Applications

- Determine the drying temperature of compound.
- To identify the sample composition.

- Identification of reactions of materials decomposition and oxidation.

3.3.5 Microhardness

Hardness tests are commonly carried out to determine the mechanical strength of materials and it correlates with other mechanical properties like elastic constants and yield stress.

Principle

Hardness measurements can be defined as macro, micro and nano according to the forces applied and displacement obtained. In the present investigation, microhardness measurement was carried out using **Leitz-Wetzlar Vicker's microhardness** tester fitted with a diamond pyramidal indenter attached to an optical microscope. Figure 3.6 shows the schematic diagram of Vicker's microhardness tester. The indentation in the form of a right pyramid with a square base and an angle of 136 degrees between opposite faces subjected to a load of 1 g to 100 kg. The full load is normally applied for 10 to 15 seconds. A hardness number is then calculated using the test load, the impression length and a shape factor for the indenter type [Gong and Li, 2000]. The depth of indentation is about 1/7 of the diagonal length. When calculating the Vicker's diamond pyramid hardness number, both diagonals of the indentation are measured and the mean of these values is used in the formula with the load used to determine the value of H_v.

The Vicker's hardness number (H_v) is calculated using the following formula

$$H_V = \frac{1.8544\ P}{d^2}\ kg/mm^2$$

Where, P being the applied load in 'kg'

d is the diagonal length of the impression in 'mm'

H_v is Vicker's hardness number

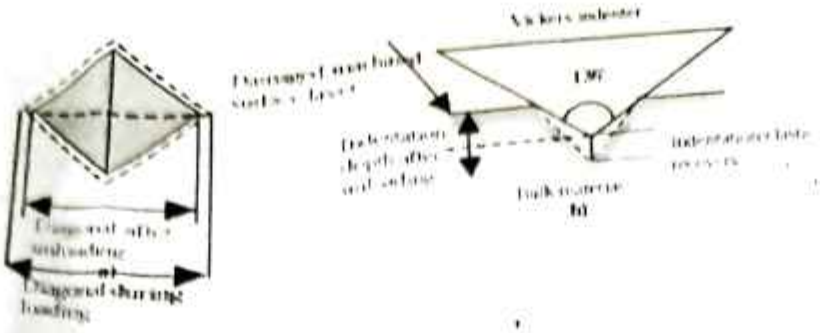

Figure 3.6 Schematic diagram of Vicker's microhardness test

Sample Preparation

As grown crystal with a size around 8 x 6 x 2 mm^3 was used in the present study. The well ordered grown crystal with flattened surface in any plane is to be selected for Vicker's hardness measurement. If the grown crystal is not polished and not in the desired shape, it has to be cut into particular shape and polished by SiC paper.

Applications

- A quantitative measure of the change in hardness can be obtained by a hardness transverse.
- Hardness measurements are used in order to determine the thickness of the hardened surface layer of this material.
- It is used to determine the crystal belongs to hard material or soft material category etc.

3.3.6 NLO Analysis

Second harmonic generation (SHG) is also called frequency doubling, a nonlinear optical process, in which photons interacting with a nonlinear material are

effectively "combined" to form new photons with twice the energy, and therefore twice the frequency and half the wavelength of the initial photons (Two photons are destroyed creating a single photon at two times of frequency)

Principle

In the present study, SHG studies have been investigated using **Kurtz and Perry powder** technique, Q-switched Nd:YAG laser emitting 1064 nm, 10 ns laser pulses having repetition rate 10 Hz with spot radius of 1 mm was used as a source for illuminating the powder sample [Kurtz and Perry, 1968]. The grown single crystal is powdered with a uniform particle size of 125–150 μm, and then packed in a microcapillary of uniform bore and exposed to the laser radiation. Figure 3.7 shows the schematic diagram of SHG method. This laser can be operated in two modes. In the single shot mode, the laser emits a single 8 ns pulse. In the multi shot mode, the laser produces a continuous train of 8 ns pulses at a repetition rate of 10 Hz and a single shot mode of 8 ns laser pulse with a spot radius of 1mm was used. A reference beam is obtained by the use of beam splitter which is placed ahead of the sample. The input laser beam was passed through an IR reflector and then directed on the microcrystalline powdered sample. The SHG was confirmed by the emission of green radiation (532 nm). The input laser energy incident on the sample was 0.68 J, an energy level optimized to cause any chemical decomposition of the sample.The intensity of the second harmonic output from the sample is compared with that of standard materials.

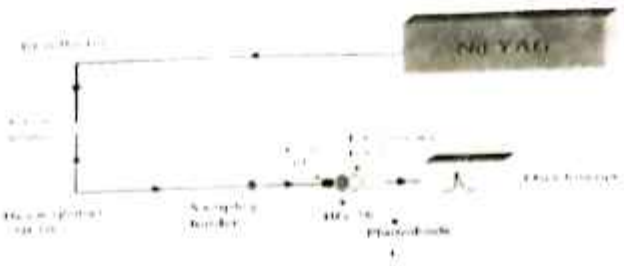

Figure 3.7 Schematic diagram of SHG method

Sample Preparation

The grown crystal is powdered using agate mortar and slieved to set uniform particle size of (125–150 μm), and then packed in a microcapillary of uniform bore and exposed to the Nd:YAG laser radiation.

Applications

- It is used as a frequency doubler in LASER technology.
- It used as phase matching in communication system.
- It used in frequency conversion etc.

CHAPTER IV

RESULTS AND DISCUSSION

Results and discussion of the grown Ammonium dihydrogen phosphate (ADP) doped potassium sulphate crystals are described in this chapter.

4.1 RESULTS AND DISCUSSION

4.1.1 Materials used

A parent compound is potassium sulphate and a doped compound is ADP. Deionized water is used as a solvent.

4.1.2 Sample preparation

The required amount of parent substance (A) and dopant substance (D) was estimated by using the formula

$$A = (M \times X \times V) / 1000 \text{ (in gram units)}$$

Where M – Molecular weight of the substance

X – Concentration in molar units

V – Required volume of the solution

Amount of potassium sulphate (A) = (174.27 x 0.8 x 100) / 1000

= 13.9416 gm

Amount of ADP (D) = (115.02 x 0.02 x 100) / 1000

= 0.23004 gm

4.1.3 Growth of ADP doped K_2SO_4 Single Crystals

Calculated amount of the reactants containing, Analar reagent (AR) of potassium sulphate (K_2SO_4) and ADP ($NH_4H_2PO_4$) were purchased from (Loba Chemie) and 2 wt% ADP is taken as a dopant quantity and deionized water was used as solvent. The calculated amount of salts were allowed to stir for more than four

hours at constant speed to achieve the homogeneity throughout the volume. After homogeneous mixing, the solutions were filtered using Whatmann 41 grade filter paper. The clear filtrate was collected in a 250 ml beaker. It was porously sealed and placed in a dust free atmosphere for slow evaporation at room temperature. Nucleation occurs within 3 days and crystals reach a large size in 14 days for all crystals. Grown crystals are very stable, colorless. The purity of the crystals was improved by successive recrystallization process. Good quality optical transparent large size crystals were selected for carrying out the measurements. The powdered sample of the crystal was also subjected to the characterization studies. The photograph of grown ADP doped K_2SO_4 single crystals are depicted in Figure 4.1.

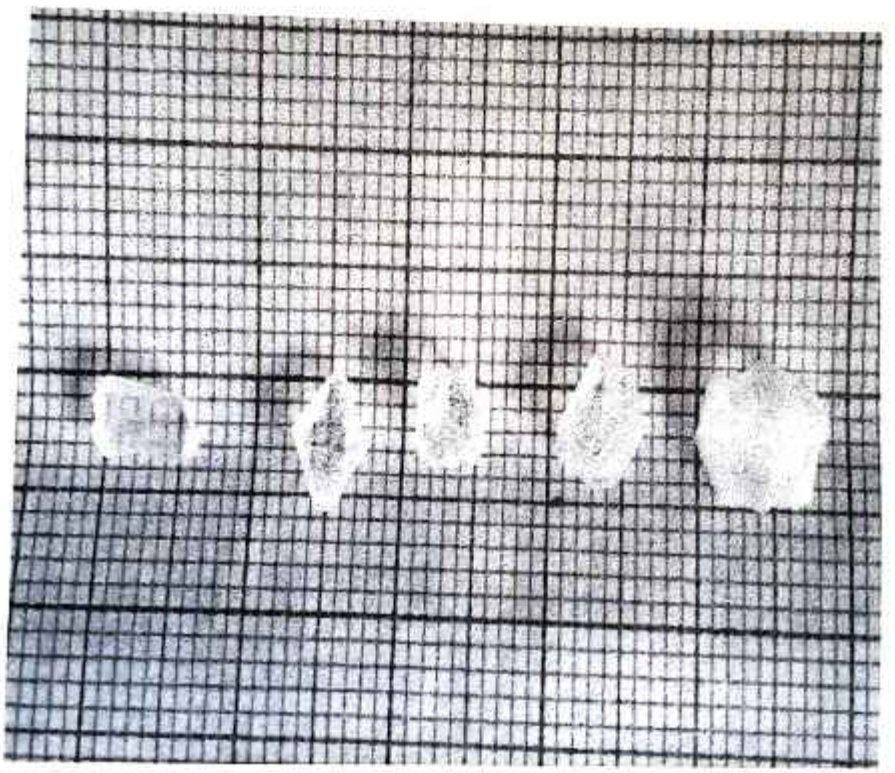

Figure 4.1 Photograph of ADP doped K_2SO_4 crystals

4.2 CHARACTERIZATION STUDIES

4.2.1 Single Crystal X-ray Diffraction

Single crystal diffractometer is most often used to determine the molecular structure of new materials. The grown crystals were subjected to single crystal X-ray diffraction to determine the unit cell parameters. In the present study, the defect free crystal of dimensions around 0.2 x 0.2 x 0.2 mm^3 is used for the single crystal analysis. Single crystal XRD were carried with MoK_α radiation (λ = 0.71073 Å). The lattice parameters of pure and doped K_2SO_4 crystals are presented in Table 4.1. It is observed from the table that the cell parameters of doped K_2SO_4 slightly differ from those of pure K_2SO_4, which may be attributed to the presence of dopant in K_2SO_4 crystals.

Table 4.1 Crystallographic data of doped K_2SO_4 crystal

Crystallographic data	ADP doped K_2SO_4	Already reported pure K_2SO_4 crystal [Tariq *et al.*, 2016]
Crystal system	Orthorhombic	Orthorhombic
Unit cell dimensions	a= 5.80 Å b = 10.13 Å c = 7.55 Å α=β=γ=90°	a= 5.746 Å b = 10.033 Å c = 7.443 Å α=β=γ=90°
Volume	444 $Å^3$	441 $Å^3$
Crystal size	10 x 7 x 2 mm^3	16 x 13 x 2 mm^3

4.2.2 Powder X-ray Diffraction

The purity and crystallinity of doped K_2SO_4 single crystal have been confirmed by recording powder X-ray diffraction pattern. The crystal was subjected to a fine powder using agate mortar and sieved into 1.0 μm sieve. A small amount of this uniform particle size powder is subjected to powder XRD analysis. To detect the diffracted X-rays from the sample an electronic detector is placed on the other side of the sample and it was scanned in the range of $10^{\circ} - 70^{\circ}$ at the scan rate of 0.04 count per minute. The indexed powder X-ray diffraction pattern is depicted in Figure 4.2. As compared with pure K_2SO_4 powder XRD pattern it is observed that there is slight shift in the peak positions and slight change in the relative intensities are due to the doping of ADP. The appearance of sharp and well-defined Bragg's peaks confirmed the crystalline nature of the grown crystal. The peak corresponding to (1 2 1) and (1 0 3) hkl plane has the maximum intensity of doped single crystal. To confirm the obtained values of unit cell parameters, powder XRD studies were also carried out for the sample. The hkl and d values were calculated and given along with the experimental d values are obtained in Table 4.2. Using the powder XRD data, the lattice parameters can be obtained using the TWOTHETA software package. The obtained value from powder XRD will be close to the obtained value from single crystal XRD studies.

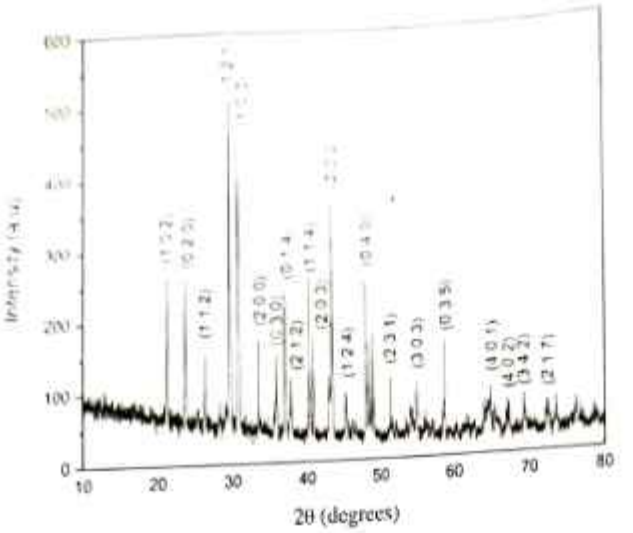

Figure 4.2 Powder XRD pattern of doped K_2SO_4 crystal

Table 4.2 Indexed powder XRD data of doped K_2SO_4crystal

2 theta (degrees)	d-spacing [Å]	Relative intensity (%)	hkl
21.33	4.16558	41.8	1 0 2
23.75	3.7452	41.33	0 2 0
29.72	3.00542	100	1 2 1
30.76	2.90622	93.35	1 0 3
30.95	2.88848	62.7	2 0 0
35.89	2.50182	17.01	0 3 0
37.01	2.42878	38.65	0 1 4
37.86	2.37639	15.97	2 1 2
40.41	2.23194	21.99	1 1 4

40.84	2.20912	26.71	2 0 3
43.39	2.08527	58.78	2 2 2
45.22	2.00513	11.57	1 2 4
48.12	1.89065	20.34	0 4 0
48.59	1.87638	16.73	2 3 1
54.93	1.67145	13.89	3 0 3
58.6	1.57525	9.48	0 3 5
64.72	1.44032	8.08	4 0 1
67.15	1.39394	5.94	4 0 2
69.32	1.35548	8.52	4 2 0
72.44	1.30461	5.83	3 4 2
73.53	1.28791	6.23	2 1 7

4.2.3 FT-IR Spectral Analysis

FT-IR spectrum of doped K_2SO_4crystal was recorded in the range 450-4000 cm^{-1} and is shown in Figure 4.3. Observed vibrational wavenumber and their assignments of doped K_2SO_4 are given in Table 4.3. Characteristic vibrational bands in the spectrum were compared with the corresponding bands of ADP. O-H stretching vibrations are observed at 3448.22 cm^{-1}, 3347.23 cm^{-1} and 3239.57 cm^{-1} which is red shifting due to inter- and intra-molecular hydrogen bonding effect [Russel, 1968]. The absorption peaks at 1384.19 cm^{-1} corresponds to the wagging vibrations of CH_2 groups present in the compound. C=O stretching vibration is observed as a strong absorption at 1569.70 cm^{-1}. Stretching vibrations of COO^- occur at 1415.92 cm^{-1} and rocking of COO^- vibrations is observed at 618.76 cm^{-1}. The peak at 485.26 is due to the O-N=P bending vibration in ADP crystal [Sunil Chaki *et al.*, 2012]. The presence

of sulfate group present in the sample is confirmed by the presence of SO_4 stretching vibration at 1115.75 cm^{-1} and 611.66 cm^{-1} (Radhika et al., 2014). The broadness was due to the hydrogen bonding interaction with adjacent molecules. From the spectra, the presence of the functional groups in the doped compound has been confirmed.

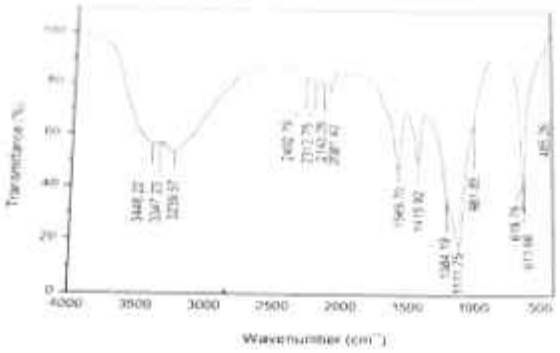

Figure 4.3 FT-IR spectrum of doped K_2SO_4 crystal

Table 4.3 Observed vibrational wavenumber and their assignments of doped K_2SO_4 crystal

Wavenumbers (cm^{-1})	Assignments
3448.22	O-H asymmetric stretching
3347.23	O-H stretching
3239.57	O-H stretching
1569.70	C=O stretching
1415.92	COO^- stretching

1384.19	CH wagging
1111.75	SO_4 stretching
981.85	C=O wagging
618.76	COO rocking
613.66	SO_4 stretching
485.26	O-N=P bending

4.2.4 UV-Vis Spectral Analysis

Optical transmission spectra were recorded in the range of 190–1100 nm. High quality grown crystal with thickness of 2 mm were used for UV-Vis spectral studies. Figure 4.4 shows the transmittance spectrum of doped K_2SO_4 crystal. The doped K_2SO_4 crystal is active in the UV-Vis region and the compound material could be viable alternative for optical materials in that entire region. An NLO material can be widely used if it has a wide transparency range. It has good transparency of about 70% with lower cut-off wavelength 390 nm. The position of peak, corresponding to n-π^* transition of the carbonyl group of the carboxyl functions. The pure K_2SO_4 has 60% transmittance with lower cut-off wavelength 350 nm [Tariq *et al.*, 2016]. It seems that the vacancies found in the undoped crystal are now filled with the dopant and hence the crystal is now free from the tensile stress. The improvement in transmission would enable better optical performance. This transparent nature in the visible region makes the doped K_2SO_4 crystal for the NLO applications. From this measurement, it is noted that there is no significant absorption in the entire visible region, which enables it to be a potential candidate for optoelectronic applications.

The dependence of optical absorption coefficient with the photon energy helps to study the band structure and the type of transition of the electron. The absorption coefficient (α) and the optical parameters such as refractive index (n), reflectance (R) and extinction coefficient (K) have been determined.

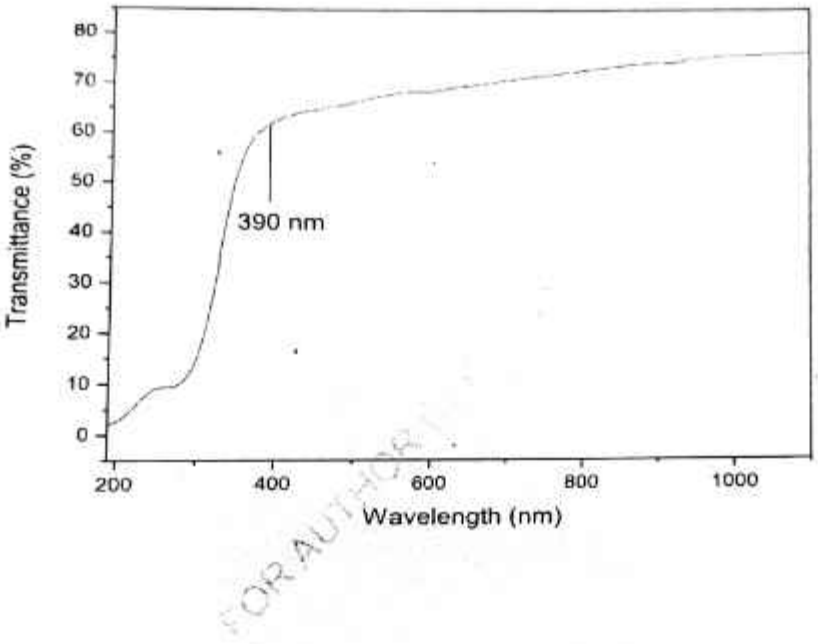

Figure 4.4 UV-Vis transmittance spectrum of doped K_2SO_4 crystal

The measured transmission (T) is used to calculate the absorption coefficient (α) based on the following relation,

$$\alpha = \frac{2.3026}{t} \log(1/T) \qquad \ldots\ldots\ldots (4.1)$$

Where, t is the thickness of the crystal.

In the high photon energy region, the energy dependence of absorption coefficient suggests the occurrence of direct band gap of the crystal obeying the following equation for high photon energies (hν) [Ashour *et al.*, 1995].

$$(\alpha h\nu)^2 = A(E_g - h\nu) \qquad \ldots\ldots\ldots (4.2)$$

Where, E_g is the optical band gap of the crystal and A is constant. The band gap of the crystal is evaluated by plotting $(\alpha h\nu)^2$ versus hν [Tauc *et al.*, 1966] as shown in Figure 4.5 and it is found to be 4.6 eV. The wide band gap of the K_2SO_4 crystal confirms the large transmittance in the visible region.

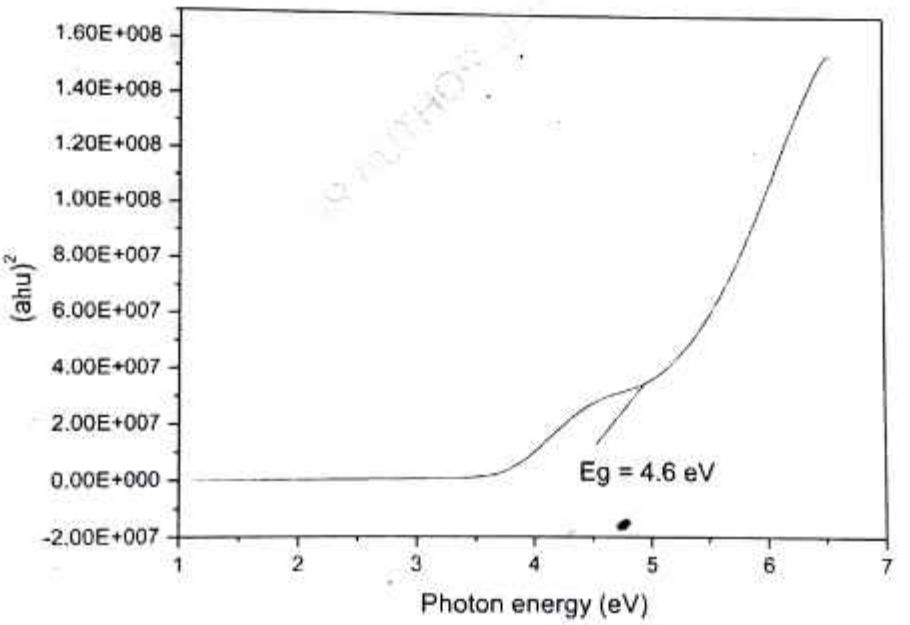

Figure 4.5 Plot of $(\alpha h\nu)^2$ vs. photon energy for doped K_2SO_4 crystal

Extinction coefficient is the fraction of light lost due to scattering and absorption per unit distance in a participating medium. In electromagnetic terms, the extinction coefficient can be explained as the decay or damping of the amplitude of the incident electric and magnetic fields. The extinction coefficient (K) is obtained from the following equation.

$$K = \frac{\alpha\lambda}{4\pi} \qquad \ldots\ldots\ldots (4.3)$$

The transmittance (T) is given by the following relation [Pankove, 1971].

$$T = \frac{(1-R)^2 \exp(-\alpha t)}{(1-R)^2 \exp(-2\alpha t)} \qquad \ldots\ldots\ldots (4.4)$$

The reflectance (R) in terms of the absorption coefficient (α) can be derived from the relations [Gupta, 1996].

$$R = \frac{\exp(-\alpha t) \pm \sqrt{\exp(-\alpha t)T - \exp(-3\alpha t)T + \exp(-2\alpha t)T^2}}{\exp(-\alpha t) + \exp(-2\alpha t)T} \qquad \ldots\ldots\ldots (4.5)$$

The refractive index (n) can be determined from reflectance data using the following relation [Omar, 1975].

$$n = \frac{-(R+1) \pm 2\sqrt{R}}{(R-1)} \qquad \ldots\ldots\ldots (4.6)$$

Extinction coefficient is the fraction of light lost due to scattering and absorption per unit distance in a participating medium. In electromagnetic terms, the extinction coefficient can be explained as the decay or damping of the amplitude of the incident electric and magnetic fields. The extinction coefficient (K) is obtained from the following equation.

$$K = \frac{\alpha\lambda}{4\pi} \qquad \ldots\ldots\ldots (4.3)$$

The transmittance (T) is given by the following relation [Pankove, 1971].

$$T = \frac{(1-R)^2 \exp(-\alpha t)}{(1-R)^2 \exp(-2\alpha t)} \qquad \ldots\ldots\ldots (4.4)$$

The reflectance (R) in terms of the absorption coefficient (α) can be derived from the relations [Gupta, 1996].

$$R = \frac{\exp(-\alpha t) \pm \sqrt{\exp(-\alpha t)T - \exp(-3\alpha t)T + \exp(-2\alpha t)T^2}}{\exp(-\alpha t) + \exp(-2\alpha t)T} \qquad \ldots\ldots\ldots (4.5)$$

The refractive index (n) can be determined from reflectance data using the following relation [Omar, 1975].

$$n = \frac{-(R+1) \pm 2\sqrt{R}}{(R-1)} \qquad \ldots\ldots\ldots (4.6)$$

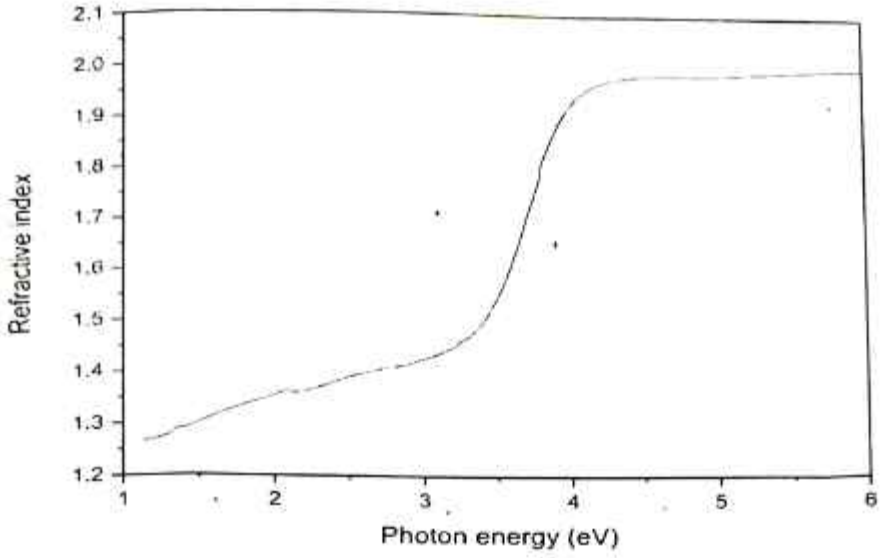

Figure 4.6 Plot of refractive index vs. wavelength for doped K_2SO_4 crystal

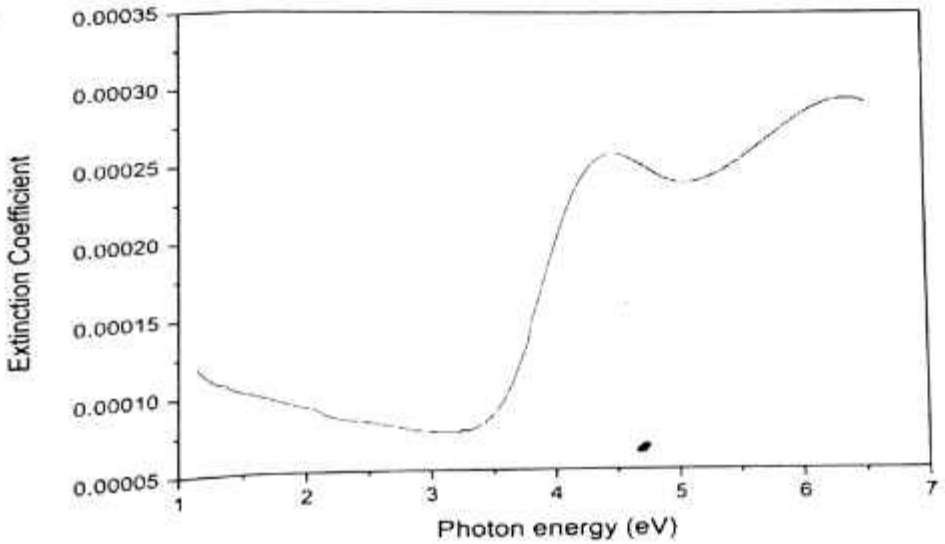

Figure 4.7 Plot of extinction coefficient vs. wavelength for doped K_2SO_4 crystal

Figures 4.6 and 4.7 represent the variation of refractive index and extinction coefficient with respect to photon energy respectively. The estimated refractive index

(n) of doped K_2SO_4 crystal from the graph is 1.37 at 532 nm. It is importantly noticed that the crystal has positive refractive index and the value increases when compared to pure K_2SO_4 with respect to energy and this indicated the focusing nature of the crystal.

From the graph, it is cleared that the extinction coefficient depends on the photon energy. Since the internal energy of the device also depends on the photon energy, by tailoring the photon energy one can achieve the desired material to fabricate the optoelectronic devices.

From the optical constants, the electric susceptibility (χ_c) can be calculated according to the relation [Gupta. 1996].

$$\varepsilon_r = \varepsilon_0 + 4\pi\chi_c = n^2\text{-}k^2 \qquad \ldots\ldots\ldots (4.7)$$

$$\chi_c = \frac{n^2-k^2-\varepsilon_0}{4\pi} \qquad \ldots\ldots\ldots (4.8)$$

Where, ε_0 is the dielectric constant in the absence of any contribution from free carriers. The estimated electric susceptibility (χ_c) is found to be 0.127 at 1100 nm.

The real and imaginary dielectric constants, ε_r and ε_i can be calculated from the following relations [Gaffar *et al.*, 2003].

$$\varepsilon_r = n^2\text{-}k^2 \text{ and } \varepsilon_i = 2nk \qquad \ldots\ldots\ldots (4.9)$$

The value of real ε_r and imaginary ε_i dielectric constants at λ=1100 nm are found to be 1.601 and 3.01×10^{-4} (no units) respectively.

4.2.5 Thermal Analysis

The TG/DSC was carried out in nitrogen atmosphere at a heating rate of 10°C /min in the temperature of room temperature to 1400°C. An Al_2O_3 (alumina) crucible

was used and it served as a reference for the sample. The mass changes in the TG curve are confirmed by DTG peaks shown in Figure 4.8.

There is a continuous weight loss from 50 °C to 1100 °C leaving behind 51% residue for doped potassium sulphate crystal. The weight loss is due to the elimination of water molecule present in the crystal. The decrease in mass may be due to the thermal decomposition of the elements present in the sample. This indicates the incorporation of ADP compound in the crystal lattice of potassium sulphate. Further the crystal is themally stable up to a temperature of 1300°C. This indicates the incorporation of ADP compound in the crystal lattice of potassium sulphate and it is suitable for possible applications in lasers where the crystal is required to withstand high temperatures.

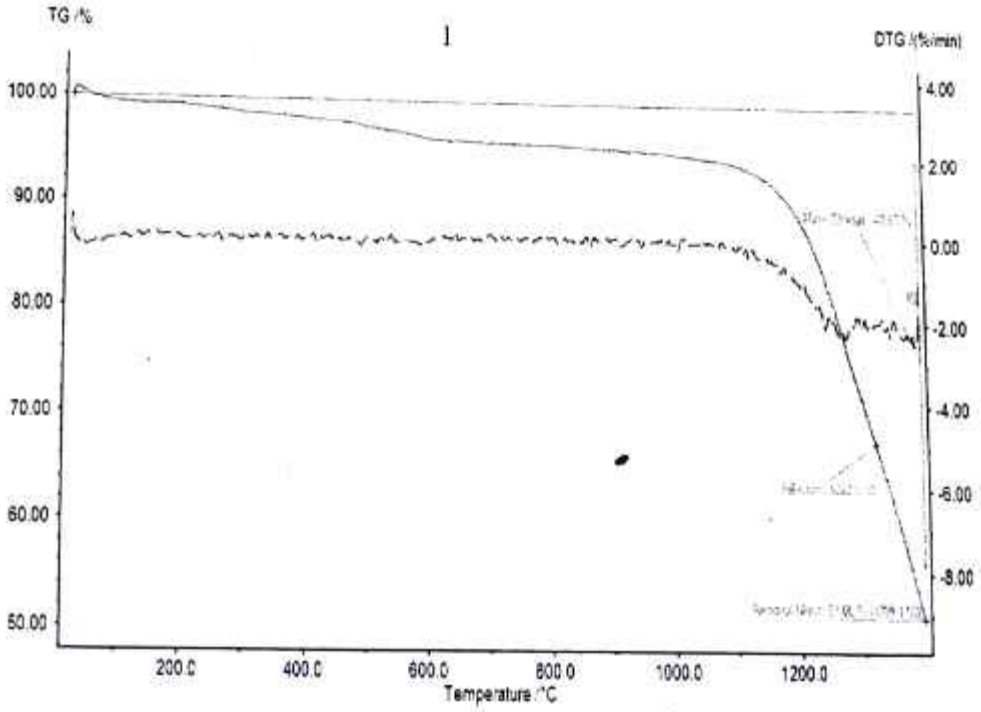

Figure 4.8 TG/DTG spectrum of doped K_2SO_4 crystal

4.2.6 Vicker's Microhardness Measurements

The Vicker's microhardness measurement was carried out on the grown crystals to assess the mechanical property. The load is applied for 25 g, 50 g and 100 g and their corresponding Vicker's hardness number is calculated. The graph is plotted between Vicker's hardness (H_v) number and load as shown in Figure 4.9. The hardness value of ADP doped K_2SO_4 single crystal is increased as compared to pure crystal for all applied loads. The relation between load and the size of indentation can be correlated using Meyer's law, $P = k_1 d^n$, where k_1 is a constant and 'n' is the Meyer's index. The slope of log p versus log d gives the work hardening coefficient (n) and it was calculated and represented in Figure 4.10. This value found is to be 3.1, which indicates that crystal belongs to soft material category. The authors have pointed out that n lies between 1.0 and 1.6 for moderately hard materials and it is more than 1.6 for soft materials [Onitsch 1956, Sahin 2005]. From these observations, it can be concluded that the doped crystal have better mechanical stability when compared to pure K_2SO_4 single crystal.

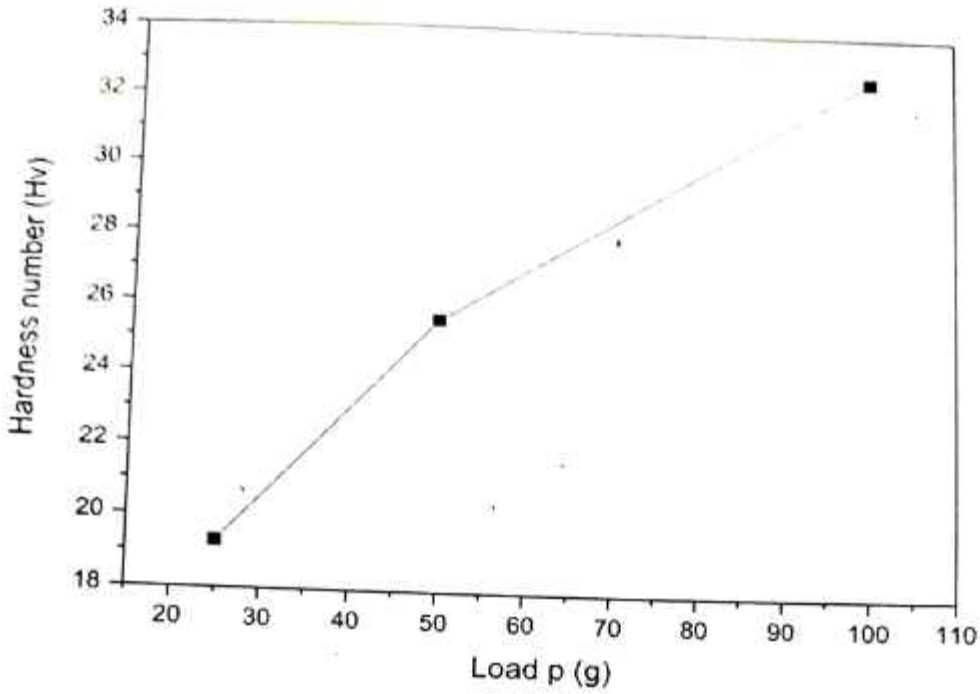

Figure 4.8 Plot of Vicker's hardness (H_v) against load (p)of doped K_2SO_4 crystal

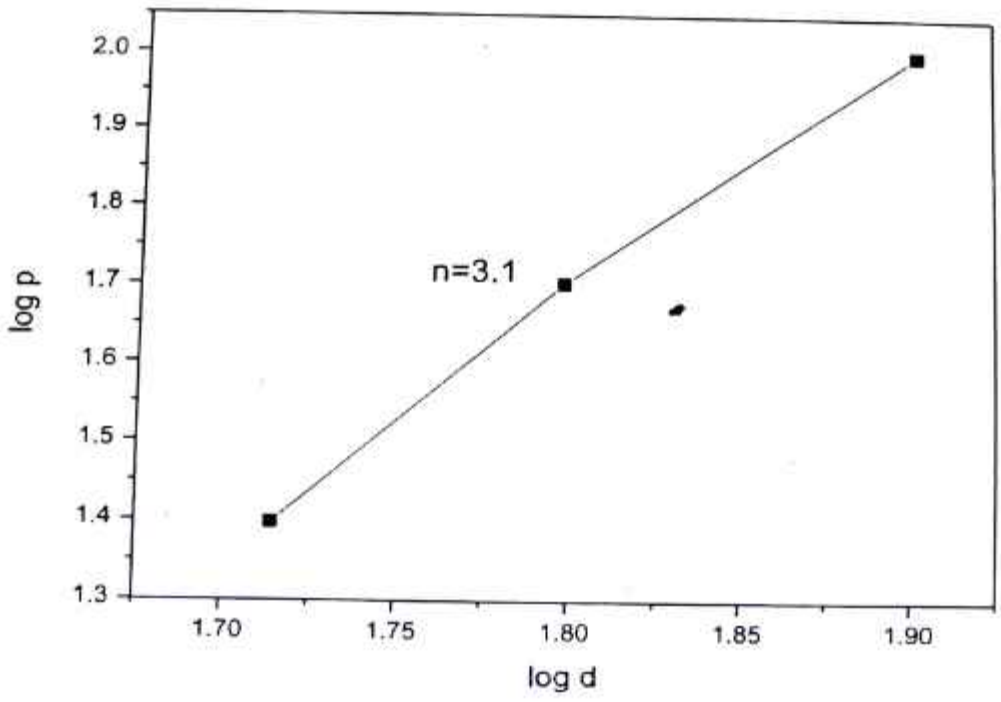

Figure 4.9 Plot of log p vs. log d of doped K_2SO_4 crystal

4.2.7 Second Harmonic Generation Studies (SHG)

To confirm the nonlinear optical property of the sample, the powder form of ADP doped K_2SO_4 crystal were subjected to NLO test obeying the Kurtz and Perry powder technique [Kurtz and Perry, 1968]. The SHG was confirmed by the emission of green radiation (λ = 532 nm). The input laser energy incident on the sample was 0.68 J, an energy level optimized to cause any chemical decomposition of the sample. The KDP is used as a reference material for the present measurement. Table 4.4 shows the comparision of SHG signals energy output. This indicate that the pure K_2SO_4 crystal have SHG efficiency is 0.308 times and doped K_2SO_4 is 0.457 times greater than that of KDP. It is found that the conversion efficiency of the doped crystal is greater than pure K_2SO_4. The efficient SHG demands specific molecular alignment of the crystal and this is to be achieved facilitating nonlinearity in the presence of dopant.

Table 4.4 Comparision of SHG signals energy output

Input power (J)	KDP reference (mJ)	Pure K_2SO_4 (mJ)	ADP doped K_2SO_4 (mJ)
0.68	8.8	3.5	5.2

CHAPTER V

CONCLUSION

The single crystals of 2 wt% ADP doped K_2SO_4 crystal was synthesized and white coloured good optical quality single crystals were grown deionized water as solvent by slow evaporation solution growth technique at room temperature. From the single crystal XRD, the doped K_2SO_4 crystal belongs to orthorhombic system. From the powder XRD, appearance of sharp and well defined Bragg's peaks confirmed the crystalline nature of the grown crystal. The peak corresponding to (1 2 1) and (1 0 3) hkl plane has the maximum intensity of doped single crystal. From the FT-IR spectra, the presence of the functional groups in the doped compound has been confirmed. The doped K_2SO_4 crystal is active in the UV-Vis region and it has good transparency of about 70% with lower cut-off wavelength 390 nm. The band gap of the crystal is found to be 4.6 eV and the estimated refractive index is found to be 1.37 at 532 nm. From the TG/DTG, the incorporation of ADP compound in the crystal lattice of potassium sulphate and it is suitable for possible applications in lasers where the crystal is required to withstand high temperatures. From the microhardness, the hardness value found is to be n = 3.1, that the crystal belongs to soft material category. The SHG efficiency of doped K_2SO_4 is 0.457 times greater than that of KDP. It is found that the conversion efficiency of the doped crystal is greater than pure K_2SO_4.

REFERENCES

1. Ananthi T. Mary Delphine S. Mary Treesa M. Krishna Priya R. and Abdul Wahab Ahmmallam. (2011). 'Growth and characterization of doped ADP crystal', Recent Research in Science and Technology, Vol. 3, No.1, pp.32-40.

2. Arulmani S. Deepa K. Indumathi N. Viktor Antony Raj M. and S Senthil S. (2017). 'Optical, thermal and electrical studies on L-malic acid doped ADP single crystals for nonlinear optical', Mechanics, Materials Science & Engineering, Vol. 9, pp.1-8.

3. Ashour A. El-Kadry N. and Mahmoud S.A. (1995), 'On the electrical and optical properties of CdS films thermally deposited by a modified source', Thin Solid Films, Vol. 269, pp.117-120.

4. Ballman A.A. Laudise R.S. and Gilrnan J.J. (1963), 'The art and science of growing crystals', John Wiley and Sons Inc.

5. Bellamy L.J. (1980), 'The Infrared Spectra of Complex Molecules:Advances infrared group frequencies', Chapman & Hall/Wiley, London/New York, Vol. 2, pp.299.

6. Bhat H.L. (2015), 'Introduction to crystal growth-principles and practice', CRC Press, Taylor and Francis Group, LLC.

7. Bolt R.J. and Bennema P. (1990), 'Potassium titanyl phosphate $KTiOPO_4$ (KTP):Relation between crystal structure and morphology', Journal of Crystal Growth, Vol. 102, pp.329-340.

8. Buce J.C. (1986), 'Crystal growth processes', Halsted Press, John Wiley and Sons, New York.

9. Buckley H.E. (1951), 'Crystal growth', John Wiley and Sons, New York.

10. Carruthers J.R. Peterson G.E. Grasso M. and Bridenbaugh P.M. (1971), 'Nonstoichiometry and Crystal Growth of Lithium Niobate', Journal of Applied Physics, Vol. 42, pp.1846-1852.

11. Chernov A. (1984), 'Modern crystallography Vol III. crystal growth', Springer-Verlag, Solid state series, Vol. 36, Berlin, 1984.

12. Clearfield A., Reibenspie J. and Bhuvanesh N. (2008), 'Principles and applications of powder diffraction', Wiley-Blacwell, pp.400.

13. Crundwell G. Phan J. and Kantardjieff K.A. (1999), 'The incorporation of a single-crystal X-ray diffraction experiment into the undergraduate physical chemistry laboratory', Journal of Chemical Education, Vol. 76, pp.1242-1245.

14. Dongfeng X. and Henryk R. (2005), 'Effect of hydrogen bonds on physical properties of ammonium dihydrogen phosphate crystals', Journal of Molecular Structure:Theochem, Vol. 716, pp.207-210.

15. Gaffar M.A. Abu El-Fadl A. and Bin Anooz S. (2003), 'Influence of strontium doping on the indirect band gap and optical constants of ammonium zinc chloride crystals', Physica B:Condensed Matter, Vol. 327, pp.43-54.

16. Goeder F.P. (1928), 'The crystal structure of potassium sulphate', Physics, Vol. 14, No.5, pp.766-771.

25. Marder S.R. Tiemann B.G. and Perry J.W. (1991), 'Materials for nonlinear optics chemical perspectives', American Chemical Society, Washington pp.280

26. Milburn G.H.W. (1973), 'X-ray crystallography an introduction to the theory and practice of single crystal structure analysis', Butterworths, pp.217.

27. Mullin J.W. and Amatavivadhana A. (1967), 'Growth kinetics of ammonium- and potassium-dihydrogen phosphate crystals', Journal of Applied Chemistry, Vol. 17, No., pp.151-156.

28. Omar M.A. (1975), 'Elementary solid state physics', Addition-Wesley Publishing Company.

29. Onitsch E.M. (1956), 'The Present Status of Testing the Hardness of Materials', Mikroskopie, Vol. 95, No., pp.12-14.

30. Pankove J.I. (1971), 'Optical processes in semiconductors', Prentice-Hall, Englewood Cliffs, NJ.

31. Radhika S. Padma C.M. Ramalingom S. and Chithambara Thanu T. (2013), 'Growth, optical, thermal, mechanical and dielectric studies of potassium sulfate crystals doped with urea', Archives of Physics Research, Vol. 4, No.1, pp.49-59.

32. Rajesh P. Boopathi K. and Ramasamy P. (2011), 'Investigation on the solubility growth, structural, optical, mechanical, dielectric and SHG behaviour of ammonium acetate doped ADP crystals', Journal of Crystal Growth, Vol. 318, No.1, pp.751-756.

33. Rajesh P. Ramasamy P. Bhagavannarayana G. and Binay Kumar. (2010). 'Growth of [100] directed ADP crystal with slotted ampoule', Current Applied Physics, Vol. 10, No.4, pp.1221-1226.

34. Rajesh P. Ramasamy P. and Bhagavannarayana G. (2013). 'Growth of ADP-KDP mixed crystal and its optical, mechanical, dielectric, piezoelectric and laser damage threshold studies', Journal of Crystal Growth, Vol. 362, pp.338-342.

35. Rajesh P. and Ramasamy P. (2009). 'Optical, dielectric and microhardness studies on [100] directed ADP crystal', Spectrochimica Acta, Vol. 74, No.1, pp.210-213.

36. Ramasamy G. and Meenakshisundaram S. (2012). 'Synthesis, characterization, crystal structure and NLO properties of a new mixed crystal potassium sodium ammonium dihydrogen phosphate $K_{0.23}Na_{0.23}(NH_4)_{0.54}H_2PO_4$', Journal of Crystal Growth, Vol. 352, pp.63-66.

37. Russel S. and Drago (1968), 'Physical Method in Inorganic Chemistry', East-West Press Pvt. Ltd, New Delhi.

38. Sadler, Pennsylvania, and Heyden (1979), 'Sadtler handbook of ultraviolet spectra, London.

39. Sahin O. Uzun O. Kolemen U. and Duzgunanducar N. (2005), 'Indentation size effect and microhardness study of β-Sn single crystals', Chinese Physics Letters, Vol. 22, pp.3137-3140.

40. Santhanaraghavan P. and Ramasamy P. (1995), 'Crystal Growth Processes and Methods', First Edition, KRI Publications Chennai, pp.304

41. Santhanaraghavan P. and Ramasamy P. (2002), 'Crystal growth processes and methods, KRI Publications, India

42. Scheel H.J. (2013), 'The development of crystal growth technology', John Wiley & Sons Ltd., Chichester.

43. Semmelroth K. Kriegor M. Pensl G. Nagasawa H. Pusche R. Hundhausen M. Ley L. Nerding M. and Strunk H.P. (2007), 'Growth of cubic SiC single crystals by the physical vapor transport technique', Journal of Crystal Growth, Vol. 308, pp.241-246.

44. Sethuraman K. Ramesh Babu R. Gopalakrishnan R. and Ramasamy P. (2006), 'Unidirectional growth of <1 1 0> ADP single crystal by SR method', Journal of Crystal Growth, Vol. 294, pp.349-352.

45. Shaikh M.A. Shirsat M.D. and Hussaini S.S. (2014), 'Investigation on the linear and nonlinear optical properties of L-lysine doped ADP crystal for NLO Applications', IOSR Journal of Applied Physics (IOSR-JAP), Vol. 6, pp.42-46.

46. Smith B. (1999), 'Infrared spectral interpretation, a systematic approach', CRC Press, Washington.

47. Sunil Chaki M. Deshpande P. Jiten P. Tailor Mahesh D. Chaudhary. and Kanchan M. (2012), 'Growth and characterization of ADP single crystal', American Journal of Condensed Matter Physics, Vol. 2, No.1, pp.22-26.

48. Sunila V. and Allen Gnana Raj G. (2014), 'Investigation on the growth and properties of (LAT)$_2$(K$_2$SO$_4$)$_3$ single crystals', Pelagia Research Library, Vol. 5, No. 2, pp.95-100.

49. Tareen J.A.K. and Kutty T.R. (1971), 'A basic course in crystallography', Proceedings of Indian Academic Sciences, Vol. 89, No.1, pp.277–282.

50. Tariq A.Al Dhahir. and Maryan E. Al Mahdawi. (2016), 'Dielectric and optical behavior for pure potassium sulfate and doped with copper and iron', Iraqi Journal of Science, Vol. 57, No.3A, pp.1699-1706.

51. Tauc J. Grigorovici R. and Vancu A. (1966), 'Optical properties and electronic structure of amorphous germanium', Physics Status Solidi B, Vol. 15, pp.627-637.

52. Vanitha D. Asath Bahadur S. and Athimoolam S. (2012), ' Crystal growth and characterization of potassium manganese nickel sulfate hexahydrate-A new UV filter', Journal of Minerals and Materials Characterization and Engineering, Vol. 11, pp.1121-1125.

53. Vere A.W. (1987), 'Crystal growth-principles and progress', Springer, Plenum Press NY and London, pp.151-253.

54. Vitalij K. Pecharsky and Peter Y. and Zavalij (2009), 'Fundamentals of powder diffraction and structural characterization of materials', Thermal methods of Analysis, Second Edition, John Wiley & Sons Canada, Limited, pp.505-1974.

55. Voronov P. Salo V.I. Puzikov V.M. Babenko V.N. Roshal A.D. and Tkachenko V.F. (2011), 'Hybrid organic-inorganic crystals based on ammonium dihydrogen phosphate and ammonium salicylate', Journal of Crystal Growth, Vol. 335, pp.84-89.

56. Walker A.C. and Buehler E. (1950), 'Growing Large Quartz Crystals', Industrial and Engineering Chemistry, Vol. 42, pp.1369-1375.

57. Willard H.H. Merritt L.L. Dean J.A. and Settle F.A. (2004), 'Instrumental Methods of Analysis', Seventh Edition, CBS Publishers and Distributers, New Delhi.

58. Xu D. (2008), 'Chemical bond simulation of KADP single crystal growth', Journal of Crystal Growth, Vol. 310, pp.7-19.